A Simple Algorithm for the Restoration of Clipped GPR amplitudes

Akshay Gulati and Robert J. Ferguson

ABSTRACT

It is common in Ground Penetrating Radar (GPR) imagery to have missing or corrupted traces. This can be either due to obstacles, noise, technical problems or economic considerations. Antenna-ground coupling is another reason for clipped amplitudes in GPR data. Most commercially available software use the famous "rubber band interpolation", which uses the spline polynomial to undo the clippings. This method is a simple polynomial based interpolation which performs declipping without considering any prior knowledge about the signal.

In this paper, a modified Projection on convex set (POCS) method is adopted for reconstruction of clipped amplitudes. Restoration of bandlimited GPR data which has undergone amplitude clipping is studied. This algorithm is tested on real GPR data which is clipped. To study the effectiveness of the technique, results obtained are compared with industry standard rubber band interpolation.

INTRODUCTION

Ground Penetrating Radar (GPR) methods are based on the same principle as seismic reflection methods. It is now a widely accepted geophysical technique. It is a non intrusive technique for detecting buried objects. The basic principle behind the GPR method is the transmission of electromagnetic energy into the earth and subsequent reflection from the interfaces of differing dielectric permitivity. The GPR transmissions for the targeted subsurface form a synthetic aperture, whose impulse response is a spatially variant curve in the space-time domain. A common set up for GPR deploys a transmitter and receiver over a targeted zone. In some applications, trans-illumination of the volume under investigation is more useful. An example of GPR response is shown in Figure 1.

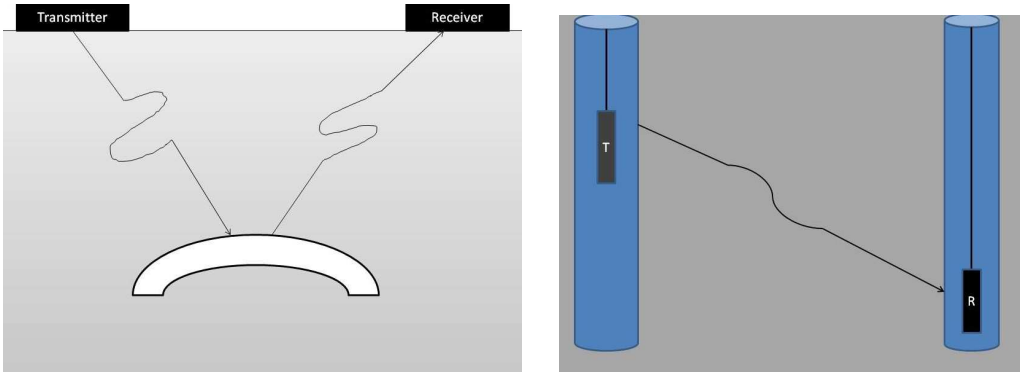

FIG. 1: Ground penetrating radar (GPR) uses radio waves to probe the subsurface of lossy dielectric materials. The modes of measurement are common. In the first, reflected or scattered energy is detected. In the second, effects on energy transmitted through the material are observed.

The response from the subsurface is extracted from the combination of all buried units within the medium. This can be inverted using number of algorithms like Synthetic Aperture Radar (SAR) image formation techniques (Gazdag, 1978) and time domain standard back projection (Feng and Sato, 2004). These algorithms require a fine grid for spatial sampling and Nyquist-rate times samples of the received signals. Hence, the data acquisition for GPR is the bottleneck of the general subsurface imaging process.

In difficult terrain, due to manual error or some technical irregularity it is possible to have missing and corrupted traces in the data. This can result in a distorted subsurface image. In the case of GPR acquisition, the GPR unit is fired at regular time intervals and data will be collected in continuous trigger mode. There is no spatial direct measurement, so instead the operator tries to maintain a constant towing speed. Variation in towing speed can not be ignored, and is evident from stretching of the GPR image, particularly at the end of the section.

If the signal is clipped, then the gap size can be large, so it can not be considered as a problem of interpolation of a regular spatial signal. The problem of interpolation of irregularly sampled signals is more complex and less well developed. It is mostly because of Shannon sampling theorem (Unser, 2000), which tells us,

"If a function $f(x)$ contains no frequency higher than a peak frequency f_o, then it is completely determined by giving its ordinates as a series of points spaced $T = \frac{2\pi}{f_o}$ seconds apart."

This restricts the extension of Shannon sampling theory to signals defined over irregular grids. Still, with some constraints, algorithms have been proposed for reconstruction of band limited (Feichtinger et al., 1995; Duijndam et al., 1999) and band unlimited signals (Naghizadeh and Sacchi, 2007a,b). These constraints limit the methods to certain applications. Large gaps in clipped GPR data is one restriction, and most band unlimited methods assume that the signal is stationary, which is generally not the case for GPR traces. Interpolation for reconstruction of seismic data (Sacchi et al., 1998; Xu et al., 2005; Liu and Sacchi, 2004; Naghizadeh and Sacchi, 2009, 2008) is performed along the lateral coordinate as we generally have irregularity of trace coverage. Here assumption that events are stationary is found to be effective.

In particular, the effectiveness of this theory and of the corresponding algorithms is restricted in the case of disparity compensated view interpolation; the derived constraints on the maximum gaps of irregular signals under perfect reconstruction conditions cannot be satisfied by irregular samples having big gaps. This restraint makes spline interpolation the only effective technique for the reconstruction in the GPR processing industry.

Other reconstruction algorithms have been proposed such as Projection on convex sets method (POCS) (Gerchberg and Saxton, 1972). This paper uses one of the hybrid method from the above categorized methods. Projection on convex sets along with non uniform fast Fourier kernel (Kunis and Potts, 2005) is used for solving the GPR clipping problem. This hybrid method will improve convergence rate and reduce the final reconstruction error. The main objective of this algorithm is to use oversampled gridding kernel, with POCS for

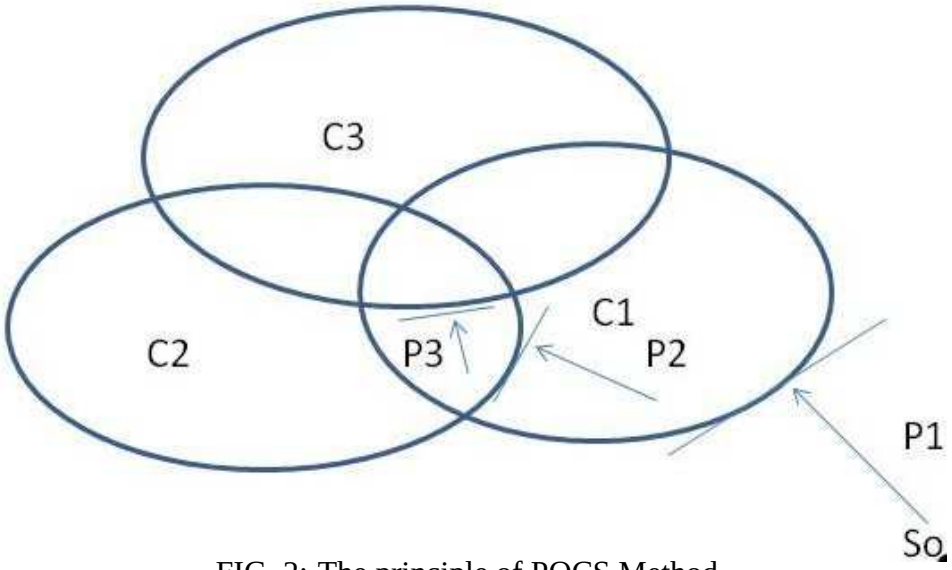

FIG. 2: The principle of POCS Method

reconstructing big gaps.

Theory

POCS method is widely used for image reconstruction. The methodology involves finding a solution as an intersection property of sets rather than by minimization of a cost function. All image constraints are represented in a Hilbert space as a series of closed convex sets $\{C_i | i = 1, 2, \cdots m\}$, then each projection is done iteratively on the intersection. In simple terms, this algorithms estimates the missing data in a Hilbert space from its known parameters.

If we have n properties of the original signal S, then each property define one of the convex sets C_i. Also, the original signal will be part of all sets as well as of the intersection of sets as in Figure 2.

$$S \in C = \cap_{i=1}^{n} C_i \tag{1}$$

Equation 1 defines n sets for n properties of signal. The initial value of the signal is projected iteratively onto the intersection of all convex sets under the projection operator P. The optimal solution will be the point lying on the boundary of the intersection. Given the projection operator P_i onto C_i,

$$S_{t+1} = P_n P_{n-1} \cdots P_1 S_t \quad t = 1, 2, \cdots \tag{2}$$

Equation 2 shows an iterative procedure for the signal with its projection operators. In Equation 2 S converges to its limiting point of the intersection C in the Hilbert space H.

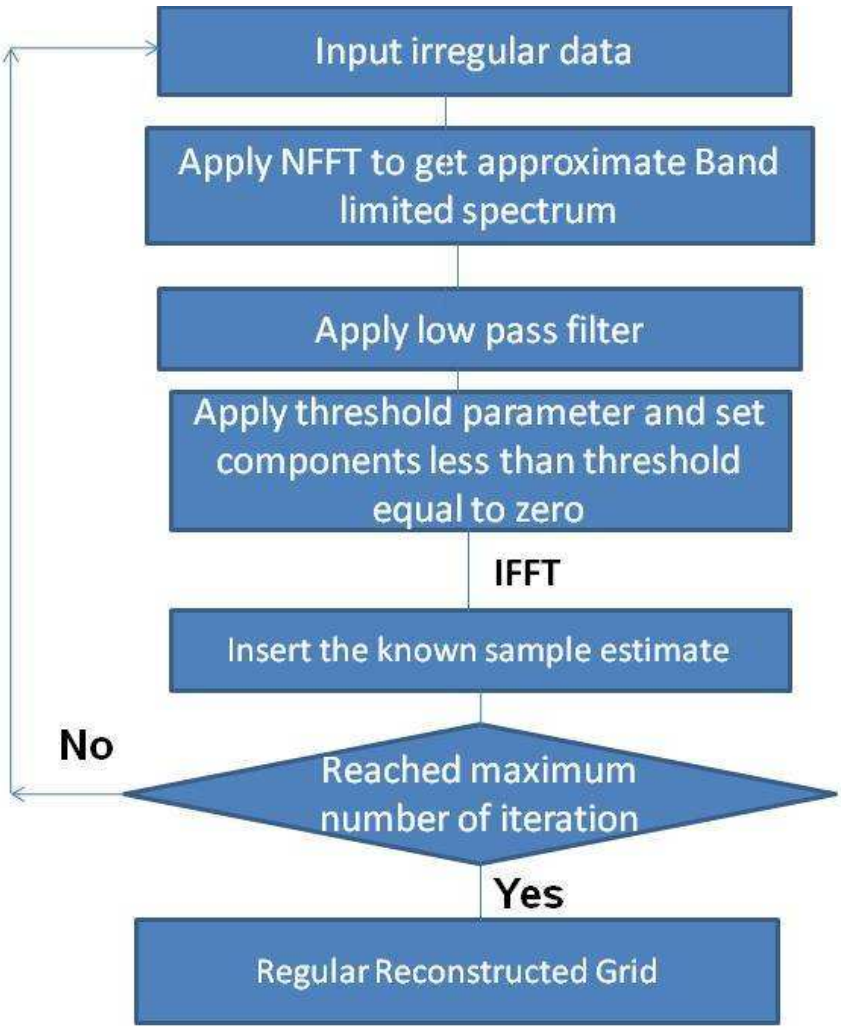

FIG. 3: flowchart

The projection operator P_i will satisfy,

$$||S - P_i S_i|| = min_{k \in C_i} ||S - k||, \tag{3}$$

where ||.|| denotes the norm in H. The limiting point can be reached from n properties of S by using Equation 2.

The first step is to grid the data onto a regular grid using a gridding kernel. In this case the gridding kernel used is the kaiser Bessel kernel (Keiner et al., 2008), which convolves with the irregular data and distribute the samples onto a regular grid. This gridding kernel, which is used as non uniform fast Fourier transform (NFFT) kernel (Kunis and Potts, 2005), acts as simple FFT when the samples are already on a regular grid. The point to be stress that, if the gaps are small then the simple FFT kernel can be applied instead of NFFT.

POCS is iterative and typically projects consecutive solutions onto consecutive properties sets. Each iteration is followed by the NFFT kernel, which is the FFT when sampling is regular enough. A threshold is applied to the Fourier domain leaving components greater

than the threshold as zero. During the first few iterations, sample points with high energy are restored. In each iterations, higher frequencies are made zero in the frequency domain. The threshold parameter enforces a cut off in amplitude which gives some amplitude to unknown values. After this, the value of known components are restored by replacing them with their true values. This will reconstruct the high frequency values. Samples will be reconstructed in each iteration (Figure 3). The whole process can be written in form of Equation 4.

$$S_k = S_{obs} + (I - S)F^{-1}T^k B(NFFT)S^{k-1} \tag{4}$$

where, S_{obs} is a original data at kth iteration. S_{obs} will keep getting updated until it finally converges to a solution. NFFT and F^{-1} represents non uniform fast Fourier transform and inverse fast Fourier transform which operates on t. S is a sampling operator that identifies known and unknown values. T^k is threshold operator with elements.

$$T^k = \begin{cases} 0, & F_{k-1} \geq l_k \\ 1, & F_{k-1} < l_k \end{cases} \tag{5}$$

Where, F_{k-1} denotes the Fourier domain representation of the reconstructed signal after the $(k-1)$th iteration. l represents the N dimensional threshold set $l = l_1, l_2, \cdots l_N$ where $l_1 > l_2 > l_N$ and N denotes the maximum number of iterations.

Experiment

The proposed reconstruction algorithm has been tested experimentally on the GPR data. The data is acquired along an ice sheet. Snow and ice are ideal GPR media because their stratification presents reflecting horizons with great continuity and interesting configurations. Due to antenna-ground coupling or some other technical issue the amplitudes in the acquired GPR data are clipped. They are clipped below -2^{15} and above $2^{15} - 1$, so there is no positive amplitude greater than 32767, and no negative amplitude below -32768.

Figure 4 shows the GPR data with a lake bottom reflection. The sampling rate for the acquired data set is 4ns. The bandwidth of data is 0-1250 MHz. Clipped amplitudes are clearly visible in Figure 4 along the top horizon. The data is compromised of 300 traces, each sampled for 750 ns. Sample traces from the data set can be seen in Figure 5, where it is clearly evident that it is clipped with maximum amplitude of 32767 and minimum amplitude of -32768.

The first step in commercial GPR processing software is the implementation of rubber band interpolation (spline interpolation). Figure 6 shows the effectiveness of spline interpolation for a GPR trace. Implementation of different interpolation technique on GPR data is carried out. Cubic interpolation along with linear and nearest neighbour interpolation is compared with spline interpolation. Cubic spline interpolation is implemented on the trace, it is a piecewise third-order polynomial passing through set of points. The result is not very effective with any other method except spline interpolation.

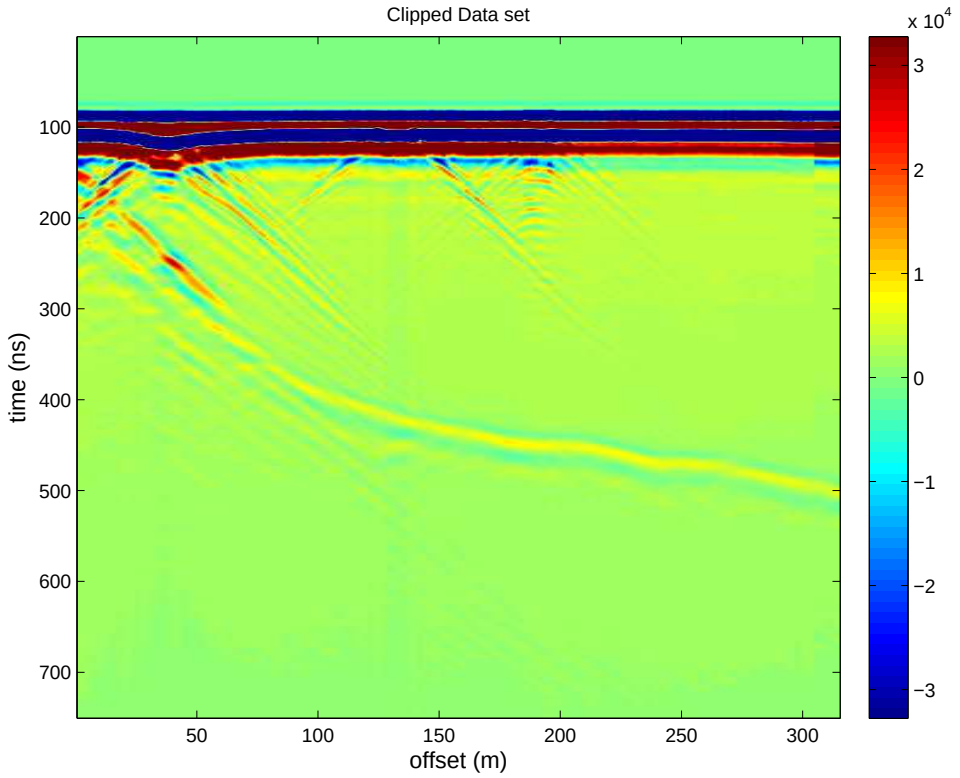

FIG. 4: Acquired GPR data with clipped horizons.

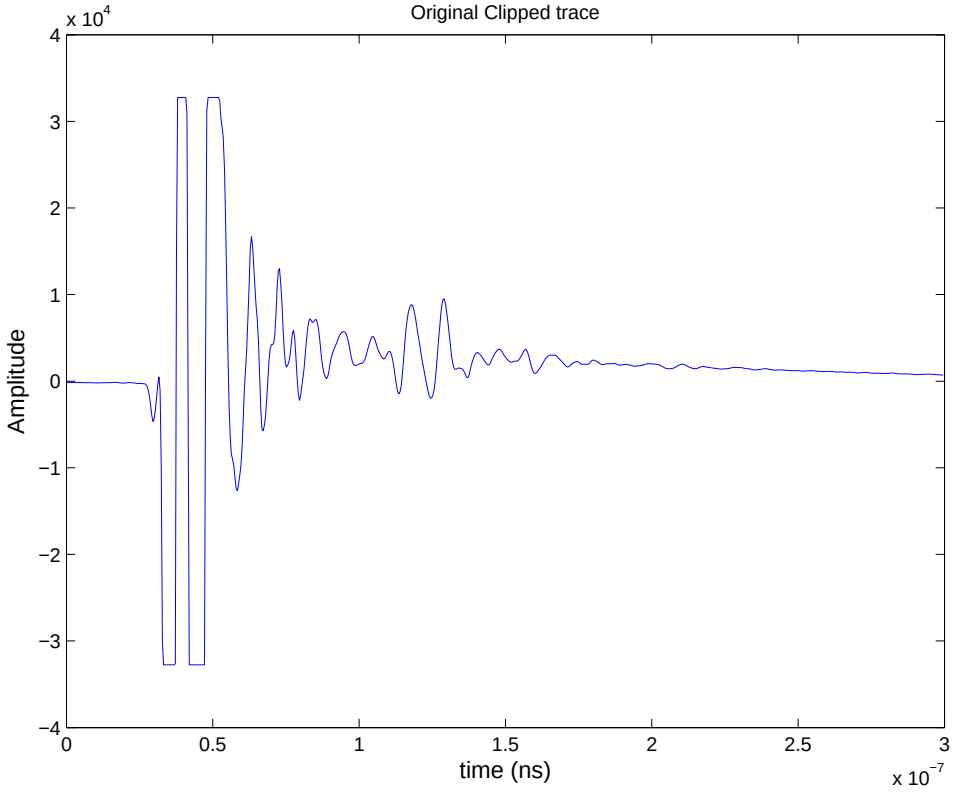

FIG. 5: Random extracted clipped trace from acquired GPR data.

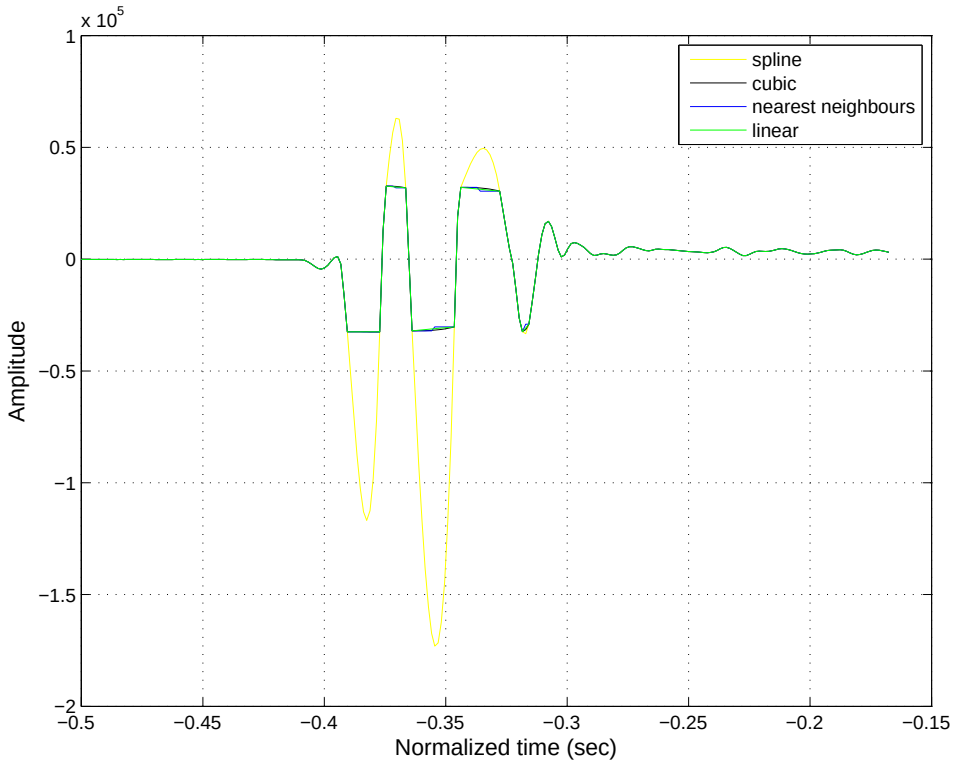

FIG. 6: Comparative study for reconstruction of clipped amplitude

This effectiveness of spline interpolation makes it a favourite module in declipping or desaturation for various GPR processing software. However, this method does not use any information from the signal. The whole reconstruction procedure is based on the fact that the interpolater is calculated on the basis of a few nearby data points. Figure 6, in which spline is use for reconstruction of single trace from GPR data, shows relatively good results as compared to other interpolators. Amplitudes are restored in Figure 7 on application of the spline based interpolation.

Effectiveness of modified POCS method is validated by comparing it with spline interpolation on different GPR traces. Figure 8a shows that for the 10th trace, there is difference in the reconstructed negative and positive clipping as compared to the spline method. Figure 8b shows a difference in all four reconstructed clippings, these four clips represent four different horizons. All of the clippings reconstructed have a significant error in both negative and positive amplitudes. Figure 8b shows another trace, where spline and Modified POCS give us similar results. Figure 8c and 8d also shows the difference in reconstructed amplitudes.

Figure 9 shows that it is not always the case that Modified POCS is constructing amplitudes smaller than the spline method. It can be seen in Figure 9a that the amplitude restored in the first clipping is higher compared to spline based technique. Also, in Figure 9c, the restored clips have higher amplitude than the splines. In both Figure 8 and 9 results obtain from our method differs from conventional spline based method.

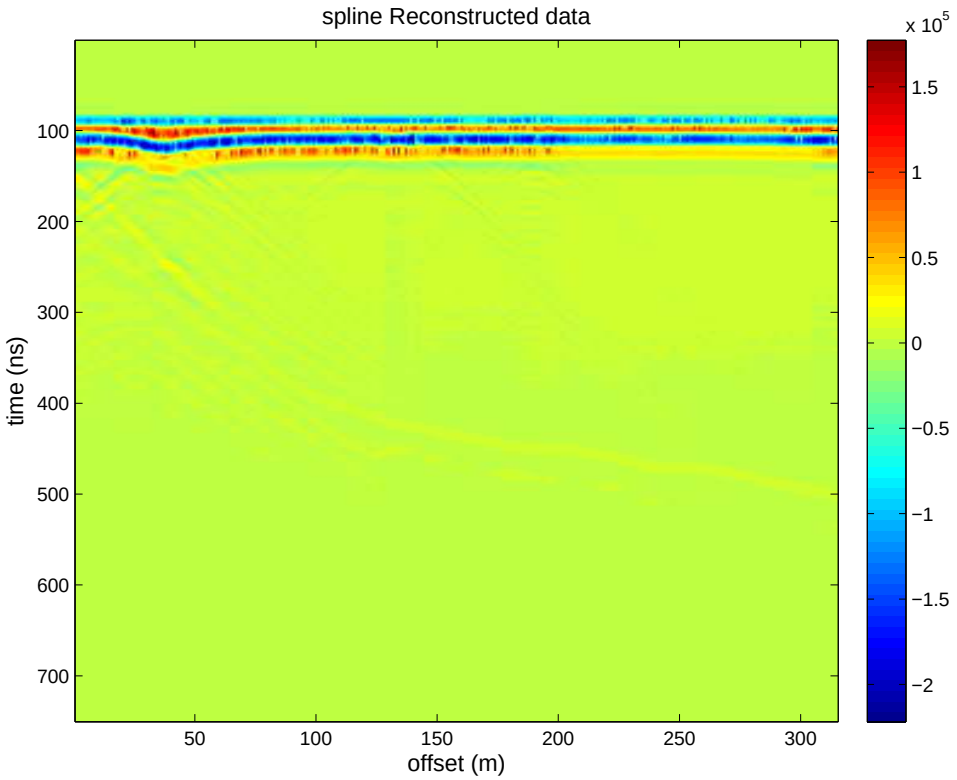

FIG. 7: Spline interpolation of clipped GPR data.

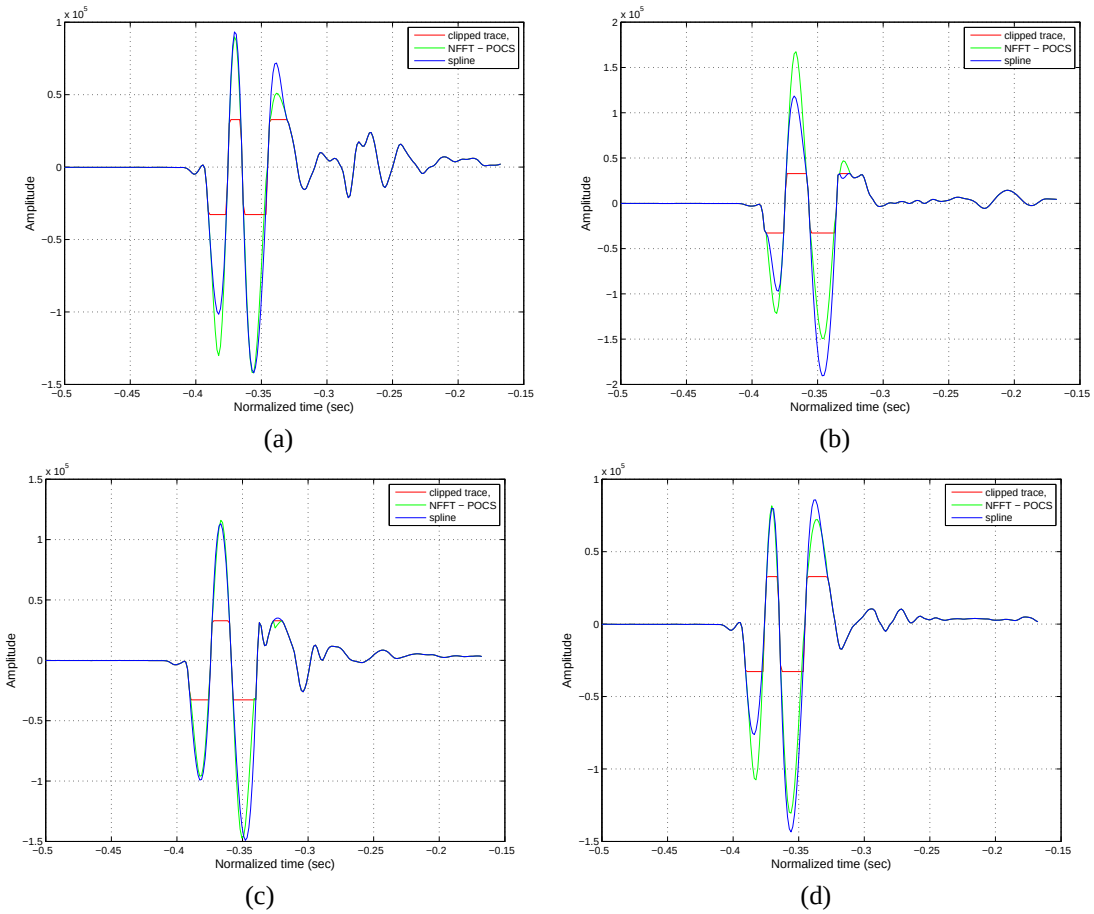

FIG. 8: Restored clipped amplitudes using Spline and Hybrid NFFT POCS. a) 10th trace from restored GPR section. b) 20th trace from restored GPR section. c) 30th trace from restored GPR section. d) 50th trace from restored GPR Section.

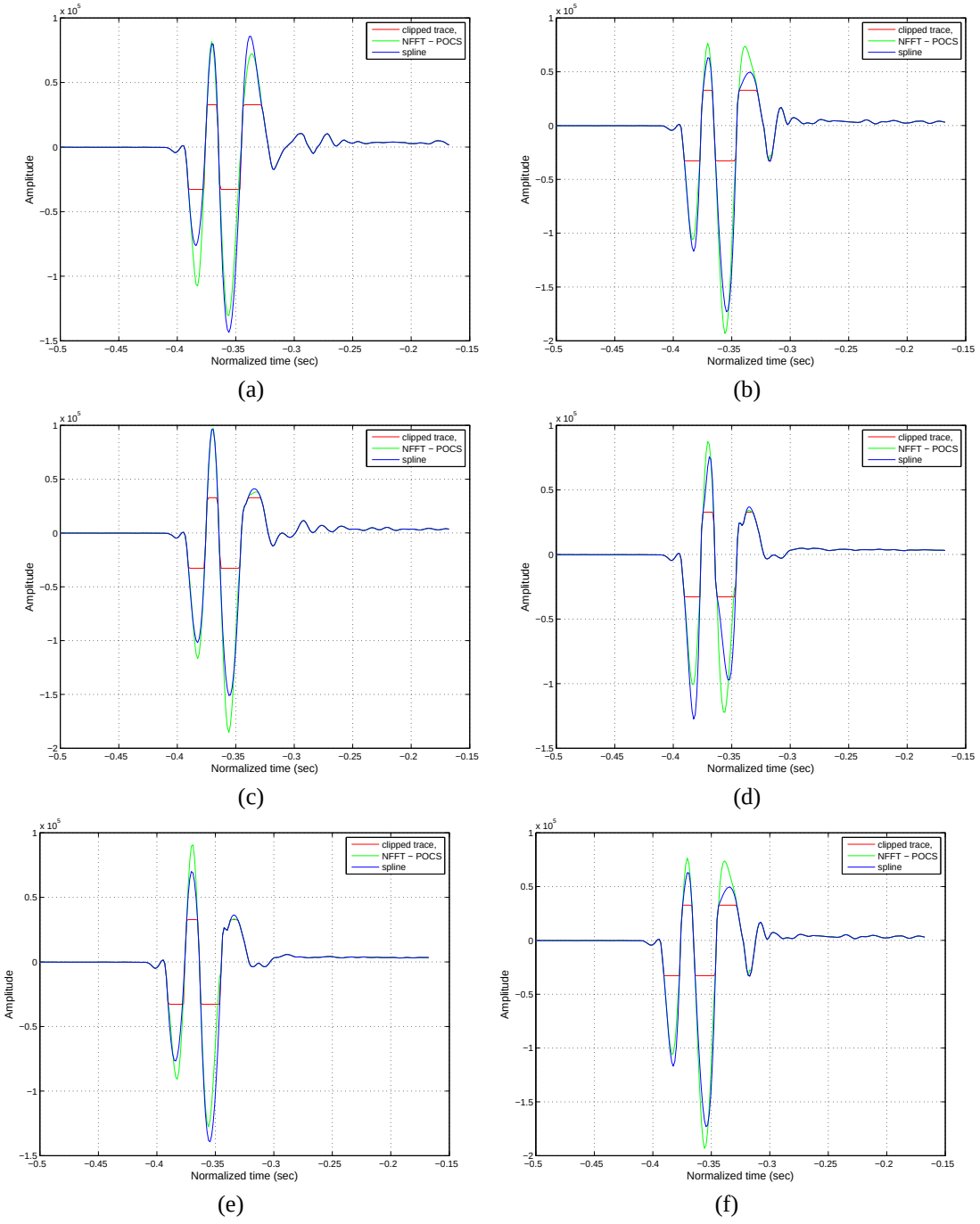

FIG. 9: Restored clipped amplitudes using Spline and Hybrid NFFT POCS. a) 100th trace from GPR Section. b) 150th trace from GPR Section. c) 200th trace from GPR Section. d) 250th trace from GPR Section. e) 280th trace from GPR Section. f) 300th trace from GPR Section.

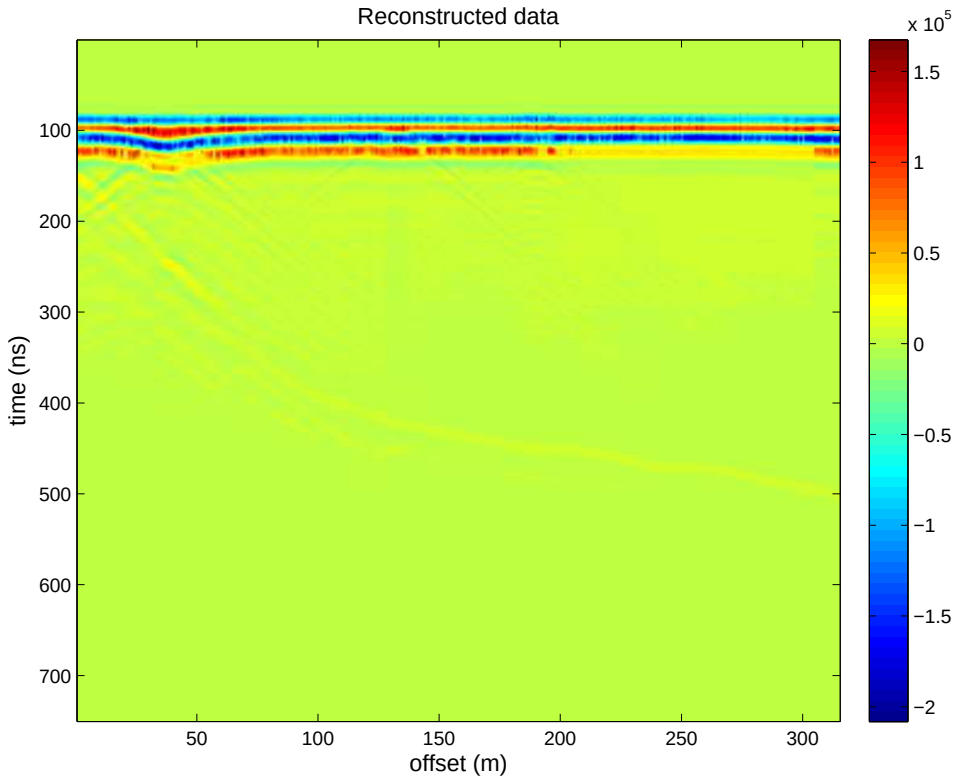

FIG. 10: Reconstructed data using Hybrid NFFT-POCS

Figure 10 shows the reconstructed GPR section. Horizons are successfully reconstructed, and the energy is continuous along the horizon, whereas the spline based reconstructed GPR section in Figure 7 seems to losing energy in the first and second horizons. It is also noted in Figures 8 and 9 that there is difference in restored amplitudes from both the methods.

We compute residuals between original clipped GPR data and POCS based reconstruction. Figure 11 shows smoothness in the restored amplitudes across the horizons. The first, second and third horizon shows constant lateral smoothness in reconstructed energy across the horizons in each layer. The residual of original clipped data and spline based method in Figure 12 shows that energy is not constant in the top horizons, which indicates the drawback of spline interpolation. Figure 13 indicates difference in the reconstructed horizons between Modified POCS and spline method, which reflects the difference in the reconstructed data.

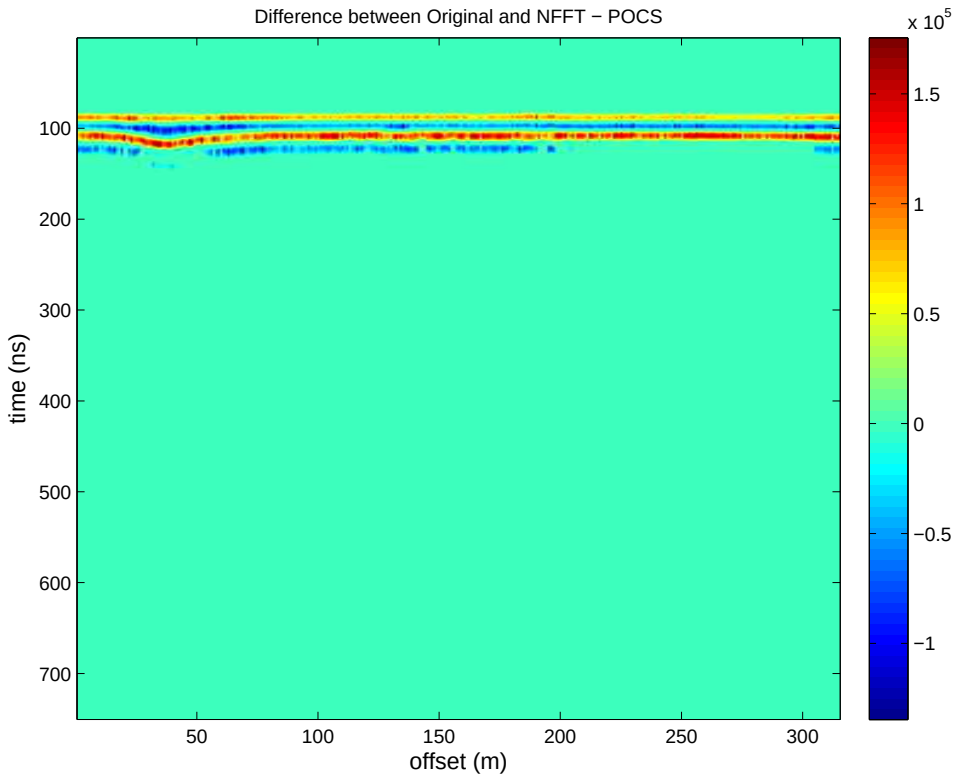

FIG. 11: Residual between original and reconstructed section using Hybrid NFFT-POCS.

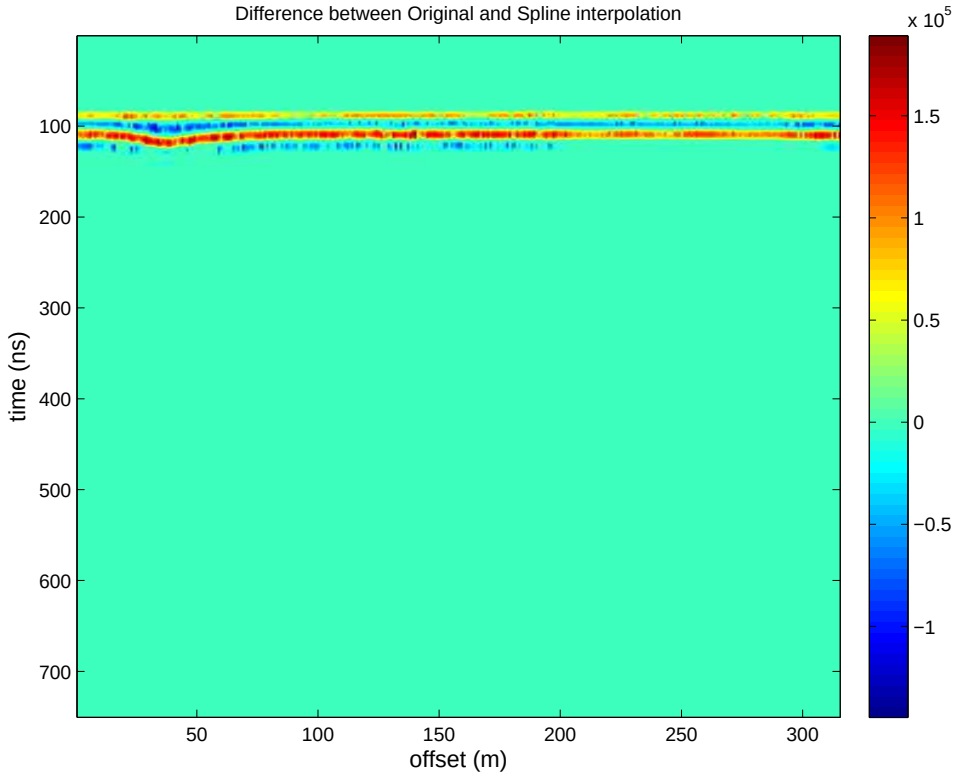

FIG. 12: Residual between original and reconstructed section using spline interpolation.

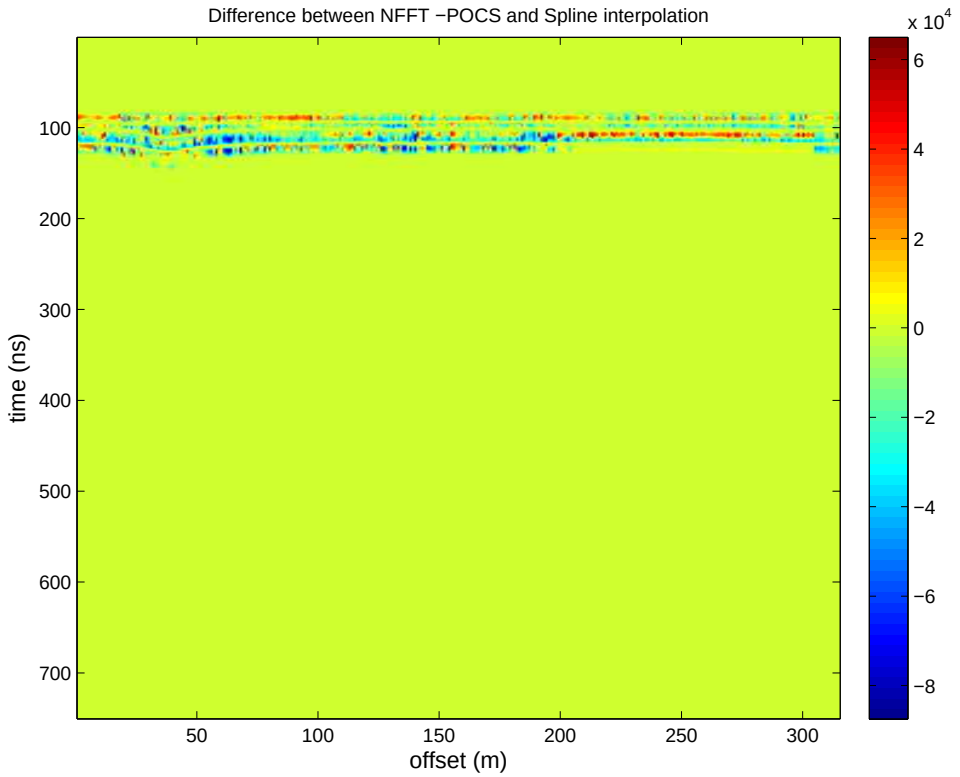

FIG. 13: Residual between restored GPR section using spline and Hybird NFFT-POCS.

CONCLUSION

In this paper, an algorithm for clipped amplitude restoration using hybrid POCS has been presented and tested. It is able to completely restore the clipped amplitudes of GPR data. Two different methods for estimating the clipping have been tested. The first one is conventional method of spline interpolation, which is largely adopted in GPR industry. The second is hybrid POCS, which uses *a priori* information from the signal to recover clipped amplitudes. A comparative study is done, which showed that Hybrid POCS is better than conventional spline interpolation. Hybrid POCS is better technique due to improved lateral continuity of the energy across the horizons in reconstructed data.

REFERENCES

Duijndam, A. J. W., Schonewille, M. A., and Hindriks, C. O. H., 1999, Reconstruction of band-limited signals, irregularly sampled along one spatial direction: Geophysics, **64**, No. 2, 524–538.

Feichtinger, H. G., Grochenig, K., and Strohmer, T., 1995, Efficient numerical methods in non-uniform sampling theory: Numerische Mathematik, **69**, 423–440.

Feng, X., and Sato, M., 2004, Prestack migration applied to gpr for lanmine detection: Invrese problems, **20**, 99–115.

Gazdag, J., 1978, Seismic migration problems and solutions: Geophysics, **43**, 1342–1351.

Gerchberg, W., R, and Saxton, O., W, 1972, A practical algorithm for the determination of phase from image and diffraction plane pictures: Optik, **35**, 237–246.

Keiner, J., Kunis, S., and Potts, D., 2008, Using nfft 3 – a software library for various nonequispaced fast fourier transforms.

Kunis, S., and Potts, D., 2005, Nfft2.0 user's manual: available online at: http://www.math.mu-luebeck.de/potts/nfft/, **version 2**, 1–22.

Liu, B., and Sacchi, M. D., 2004, Minimum weighted norm interpolation of seismic records: Geophysics, **69**, No. 6, 1560–1568.

Naghizadeh, M., and Sacchi, M. D., 2007a, Multistep autoregressive reconstruction of seismic records: Geophysics, **72**, No. 6, V111–V118.

Naghizadeh, M., and Sacchi, M. D., 2007b, Reconstruction of irregularly sampled, aliased data with multistep autoregressive operators: SEG Technical Program Expanded Abstracts, **26**, 2580–2583.

Naghizadeh, M., and Sacchi, M. D., 2008, Sampling functions and sparse reconstruction methods: EAGE Conference, Rome, Italy.

Naghizadeh, M., and Sacchi, M. D., 2009, Sampling considerations for band-limited fourier reconstruction of aliased seismic data: EAGE Conference, Amsterdam, Netherlands.

Sacchi, M. D., Ulrych, T. J., and Walker, C. J., 1998, Interpolation and extrapolation using a high-resolution discrete fourier transform: IEEE Transaction on Signal Processing, **46**, No. 1, 31–38.

Unser, M., 2000, Sampling - 50 years after shannon: Proceedings of the IEEE, **88**, No. 4, 569–587.

Xu, S., Zhang, Y., Pham, D., and Lambare, G., 2005, Antileakage fourier transform for seismic data regularization: Geophysics, **70**, No. 4, V87–V95.